# Measurement report: Emission factors of $NH_3$ and $NH_x$ for wildfires and agricultural fires in the United States

Laura Tomsche[1,2,3,+], Felix Piel[4,5,6], Tomas Mikoviny[5], Claus J. Nielsen[5], Hongyu Guo[7], Pedro Campuzano-Jost[7], Benjamin A. Nault[8], Melinda K. Schueneman[7], Jose L. Jimenez[7], Hannah Halliday[9], Glenn Diskin[2], Joshua P. DiGangi[2], John B. Nowak[2], Elizabeth B. Wiggins[1,2], Emily Gargulinski[10], Amber J. Soja[2,10], and Armin Wisthaler[4,6]

[1]Universities Space Research Association, Columbia, MD, USA
[2]NASA Langley Research Center, Hampton, VA, USA
[3]Institute of Atmospheric Physics, German Aerospace Center, Oberpfaffenhofen, Germany
[4]Department of Chemistry, University of Oslo, Oslo, Norway
[5]IONICON Analytik GmbH, Innsbruck, Austria
[6]Institut für Ionenphysik und Angewandte Physik, Universität Innsbruck, Innsbruck, Austria
[7]Department of Chemistry and Cooperative Institute for Research in Environmental Sciences (CIRES), University of Colorado, Boulder, CO, USA
[8]Center for Aerosol and Cloud Chemistry, Aerodyne Research, Inc., Billerica, MA, USA
[9]US Environmental Protection Agency, Durham, NC, USA
[10]National Institute of Aerospace, Hampton, VA, USA
[+]now at: Institute of Atmospheric Physics, Johannes-Gutenberg University Mainz, Mainz, Germany

*Correspondence to*: Armin Wisthaler (armin.wisthaler@kjemi.uio.no)

**Abstract.** During the 2019 Fire Influence on Regional to Global Environments and Air Quality (FIREX-AQ) study, the NASA DC-8 carried out *in situ* chemical measurements in smoke plumes emitted from wildfires and agricultural fires in the contiguous US. The DC-8 payload included a modified proton-transfer-reaction time-of-flight mass spectrometer (PTR-ToF-MS) for the fast measurement of gaseous ammonia ($NH_3$) and a high-resolution time-of-flight aerosol mass spectrometer (AMS) for the fast measurement of submicron particulate ammonium ($NH_4^+$). We herein report data collected in smoke plumes emitted from six wildfires in the Western US, two prescribed grassland fires in the Central US, one prescribed forest fire in the Southern US, and 66 small agricultural fires in the Southeastern US. Smoke plumes contained double to triple digit ppb levels of $NH_3$. In the wildfire plumes, a significant fraction of $NH_3$ had already been converted to $NH_4^+$ at the time of sampling ($\geq 2$ h after emission). Substantial amounts of $NH_4^+$ were also detected in freshly emitted smoke from corn and rice field fires. We herein present a comprehensive set of emission factors of $NH_3$ and $NH_x$, with $NH_x = NH_3 + NH_4^+$. Average $NH_3$ and $NH_x$ emission factors for wildfires in the Western US were $1.86 \pm 0.75$ g kg$^{-1}$ of fuel burned and $2.47 \pm 0.80$ g kg$^{-1}$, respectively. Average $NH_3$ and $NH_x$ emission factors for agricultural fires in the Southeastern US were $0.89 \pm 0.58$ g kg$^{-1}$ and $1.74 \pm 0.92$ g kg$^{-1}$, respectively. Our data show no clear inverse correlation between modified combustion efficiency (MCE) and $NH_3$ emissions. The observed ~~Importantly, we found that~~ $NH_3$ emissions ~~in ambient sampling~~ were significantly higher than ~~observed~~ measured in previous laboratory experiments ~~with similar fuel types~~ in the FIREX FireLab 2016 study.

## 1 Introduction

Ammonia ($NH_3$) is an important trace gas in the Earth's atmosphere that is mostly emitted from agriculture, traffic, the oceans and biomass burning. In the presence of acids, $NH_3$ rapidly partitions to aerosol particles, which in turn impact air quality and climate (Seinfeld and Pandis, 2016). In much of the atmosphere, $NH_3$ exhibits a major influence on particle acidity (pH), which is a major controlling parameter for many important aerosol physical and chemical processes (*e.g.*, Pye et al., 2020; Nault et al., 2021). $NH_3$ is also the largest contributor to deposition of nitrogen from the atmosphere to soil and vegetation, causing surface water eutrophication, soil acidification, and ultimately biodiversity loss (*e.g.*, Bobbink and Higgs, 2014).

Fires emit $NH_3$ predominantly during smoldering combustion, which occurs at low temperatures (*e.g.*, Lobert et al., 1990; Yokelson et al., 1996, 1997; Goode et al., 1999; McMeeking et al., 2009; Burling et al., 2010; Roberts et al., 2020). $NH_3$ is typically the third most abundant nitrogen compound (after $N_2$ and NO) and the most abundant reduced nitrogen compound emitted from fires (Lobert et al., 1990; Roberts et al., 2020; Lindaas et al., 2021).

An important parameter for investigating the atmospheric impact of $NH_3$ is the emission factor, $EF_{NH_3}$, which is the mass of $NH_3$ (in g) that is emitted per mass of fuel burned (in kg). Several literature reviews (Andreae and Merlet, 2001; Akagi et al, 2011; Andreae, 2019; Prichard et al., 2020) report $EF_{NH_3}$ values for different types of fire fuels. A closer look at the literature reveals that emissions from fuels that are typical of the United States (US) have mostly been studied in the laboratory (*e.g.,* Yokelson et al., 1996; McMeeking et al., 2009; Burling et al., 2010; Stockwell et al., 2015; Selimovic et al., 2018; Roberts et al., 2020). Previous work has shown that laboratory fires may not realistically simulate fires occurring in the real world due to different burning conditions and the lack of heterogeneity in fuels (*e.g.*, Yokelson et al., 2013; Hodshire et al., 2019). Only very few studies have reported $EF_{NH_3}$ derived from measurements carried out in the field (*e.g.*, Lindaas et al., 2021).

The limited availability of field data is mostly because $NH_3$ is difficult to measure. $NH_3$ is a "sticky" molecule that easily adsorbs onto inlet and instrumental surfaces. This makes fast airborne measurements of $NH_3$ particularly challenging. Müller et al. (2014; see Supplement) have shown that proton-transfer-reaction time-of-flight mass spectrometry (PTR-ToF-MS) can be used for airborne $NH_3$ measurements, although with some limitations tied to a relatively slow time response and a poor detection limit due to a large intrinsic background. The conventional University of Innsbruck PTR-ToF-MS instrument has measured $NH_3$ with such constraints in previous airborne studies (Sun et al., 2015; Kelly et al., 2018; Guo et al., 2021; Da Pan et al., 2021).

The Fire Influence on Regional to Global Environments and Air Quality (FIREX-AQ) study was a joint NOAA/NASA effort to investigate the atmospheric impact of wildfires and agricultural fires in the contiguous US (Warneke et al., 2023). In summer 2019, the NASA DC-8 Airborne Science Laboratory performed *in situ* measurements in smoke plumes emitted from wildfires in the Western US and agricultural fires in the Southeastern US. The aircraft payload included a modified PTR-ToF-MS instrument that was optimized for the fast measurement of $NH_3$. It also included an aerosol mass spectrometer

(AMS) for fast measurement of submicron particulate ammonium ($NH_4^+$). This allowed us to measure and report a set of emission factors of $NH_3$ and $NH_x$, with $NH_x = NH_3 + NH_4^+$, for different types of fires.

## 2 Methods

### 2.1 FIREX-AQ

The FIREX-AQ experiment has been described in detail by Warneke et al. (~~2022~~2023~~2~~). During the 2019 field campaign, $NH_3$ and $NH_4^+$ were measured aboard the NASA DC-8 in smoke plumes emitted from six wildfires in the Western US (Shady, Williams Flats, Castle, Ridge Top, Mica/Lick Creek, Horsefly), two prescribed grassland fires in the Central US (Hickory Ridge State Wildlife Management Area, Tallgrass Prairie National Preserve), and one prescribed forest fire in the Southern US (Black Water River State Forest) (. Fig. 1)~~A map showing the location of these fires is given in the Supplement (Fig. S1).~~
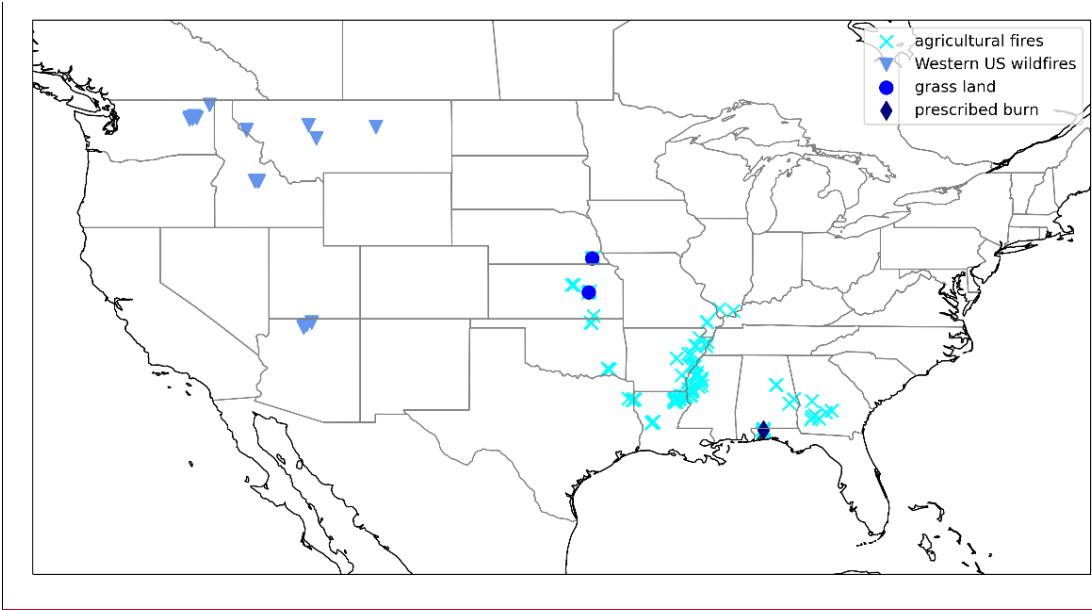
**Figure 1: Location of the fires that were sampled by the NASA DC-8 during the FIREX-AQ 2019 campaign and for which $NH_3$ and $NH_4^+$ data were obtained.**

~~Vegetation and fuel type information is summarized in Tab. S1. Information about fuel types was obtained from the 30 m Fuel Characteristic Classification System (FCCS; Ottmar et al., 2007), the 30 m Cropland Data Layer classification 2019 dataset, and ground intelligence.~~Several downwind transects were typically flown in the smoke plumes emitted from the wildfires. In addition, the NASA DC-8 sampled smoke plumes from a large number of agricultural fires in the Southeastern US. These small plumes were typically sampled twice in perpendicular direction. We successfully measured $NH_3$ and $NH_4^+$ in plumes emitted from 66 agricultural fires.

85 Vegetation and fuel type information is summarized in Tab. S1. Information about fuel types was obtained from the 30 m Fuel Characteristic Classification System (FCCS; Ottmar et al., 2007), the 30 m Cropland Data Layer classification 2019 dataset, and ground intelligence.

## 2.2 Instrumentation

A modified PTR-ToF-MS instrument was used for fast-response measurements of $NH_3$ aboard the NASA DC-8 during FIREX-
90 AQ. The conventional airborne PTR-ToF-MS analyzer has been described in detail by Müller et al. (2014). Only the modifications pertinent to the fast measurement of $NH_3$ are thus described here.

For reducing the instrumental $NH_3$ background, 12-25 standard cubic centimeters per minute (sccm; "standard" herein means referenced to a temperature of 273.15 K and a pressure of 101325 Pa) of ultra-pure helium (6.0; Praxair Inc., Danbury, CT, US) were introduced into the source drift region between the drift tube and the ion source. This reduced the backflow of
95 nitrogen into the plasma region and suppressed $NH_3$ formation in the plasma (Müller et al., 2020, and references therein). The instrumental $NH_3$ background was thereby reduced from triple digit to low single digit ppb levels.

For improving the instrumental time response to $NH_3$, all stainless-steel parts in the drift tube were surface-passivated with a functionalized hydrogenated amorphous silicon coating (Piel et al., 2021), and the drift tube was heated to 120 °C. Surface passivation and heating significantly reduces the adsorption of $NH_3$ to instrumental surfaces, lowering the instrumental
100 response time to ~2 seconds (see Figure 4 of Piel et al., 2021).

A series of inlet configurations were tested during the initial phase of the FIREX-AQ campaign. The fastest response to $NH_3$ was achieved when air was sampled at a flow rate of ~60 standard liters per minute (slpm) through a heated Teflon PFA tube (length: ~2 m, inner diameter: 3.96 mm, wall temperature: 60 °C). Evaporation of ammonium nitrate particles in the main sampling line was not investigated, but is believed to be small due to the short sample residence time (<25 ms). For inertially
105 separating particles from the analyte air, a small flow was subsampled from the main inlet line in rearward direction and directed into the drift tube through a Teflon PFA tube (length: ~10 cm, outer diameter: 3.175 mm, temperature: 120 °C). The subsampling flow was set to ~250 sccm via a pinch valve applied on the PFA tube. An $NH_3$ time response of a few seconds was ultimately achieved (see Results section).

We performed three types of calibrations in the field: i) periodic in-flight Since in field calibrations using a dynamically diluted
110 calibration standard in a pressurized cylinder (10 ppm $NH_3$ in $N_2$; Praxair Distribution Inc., Lancaster, CA, U.S.A.), ii) a ground-based calibration using a dynamically diluted calibration standard in a pressurized cylinder (2.7 ppm $NH_3$ in $N_2$; provided by NOAA's Chemical Sciences Laboratory), iii) a ground-based calibration using an $NH_3$ permeation source (provided by NOAA's Chemical Sciences Laboratory). While results from the cylinder-based calibrations were in good agreement, the permeation tube based calibration yielded an instrumental response factor that was a factor of two higher. For
115 resolving this inconsistency with different methods ($NH_3$ in $N_2$ standard gas cylinder, permeation calibration device, cross-calibration with a Picarro G2103 $NH_3$ analyzer) were inconsistent, we carried out an extensive post-mission $NH_3$ calibration

in the laboratory. For that purpose, an artificial atmosphere ($NH_3$ in air) was generated in a 250 L environmental ("smog") chamber equipped with a Fourier Transform Infrared (FT-IR) spectrometer (Bruker IFS 66v/S). The concentrations of $NH_3$ (accuracy: ±5 %) were determined from the FT-IR spectra (120 m path length, 0.125 $cm^{-1}$ spectral resolution) in a global non-linear least squares spectral fitting procedure (Griffith, 1996) employing the absolute cross sections of $NH_3$ (Gordon et al., 2017). The instrumental response factor derived from the post-mission calibration agreed to within ±15 % with the response factors obtained during the in-flight calibrations. We concluded that the permeation rate determined in pre-campaign laboratory measurements had changed in the field. The estimated accuracy of the reported $NH_3$ mixing ratios is ±15 %. We note that this accuracy estimate is not valid when $NH_3$ mixing ratios abruptly changed and inlet/instrument surfaces were not equilibrated.

Submicrometer (50% cutoff size for a vacuum aerodynamic diameter ~1 µm (about 850 nm geometric diameter for most fire plumes based on in-field calibrations) $NH_4^+$ was measured by an Aerodyne high-resolution time-of-flight AMS instrument (DeCarlo et al., 2006; Canagaratna et al., 2007), with a time resolution of up to 10 Hz time. The accuracy ($2\sigma$) of the $NH_4^+$ data is estimated to be ±34 % (Bahreini et al., 2009), while the detection limit was typically much smaller (25 ppt at 1 Hz in clean air, ~200 ppt in fire plumes). The inlet flow was optimized to allow for near real time sampling (0.3 s residence time) and to minimize particle volatilization in the inlet. We note that, based on the current state of knowledge, the AMS $NH_4^+$ data collected in fresh smoke plumes suffer from a minor ($\leq 20\%$) positive interference from reduced organic nitrogen compounds, which are known to be abundant constituents of biomass burning particles (*e.g.*, Mace et al., 2003). A general correction is still under development based on positive matrix factorization (PMF) analysis.

Carbon monoxide (CO) and methane ($CH_4$) were measured by the Differential Absorption Carbon Monoxide Measurement (DACOM) instrument (Sachse et al., 1991), which is based on mid-infrared wavelength modulation spectroscopy. The uncertainty in the CO data is 2.1 ± 0.2 ppb; the uncertainty for $CH_4$ is about 1 %. Carbon dioxide ($CO_2$) was measured by a LICOR model 7000 analyzer (Vay et al., 2009), which is based on nondispersive infrared absorption spectroscopy. For $CO_2 <$ 500 ppm, the accuracy is 0.25 ppm and the precision is 0.1 ppm, while for higher mixing ratios the total uncertainty is about 2 %.

## 2.3 Emission factor, modified combustion efficiency

We used the carbon mass balance method for calculating $EF_{NH_3}$ (Yokelson et al., 1996; 1999). The underlying assumption is that the carbon in the fire fuel is predominantly emitted as $CO_2$, CO and $CH_4$. $EF_{NH_3}$ (in g $kg^{-1}$) is thus described by the simplified equation (1):

$$EF_{NH_3} = \frac{\Delta NH_3}{\Delta CO_2 + \Delta CH_4 + \Delta CO} \times \frac{17}{12} \times F_c \times 1000 \quad (1)$$

$\Delta$ is the above background mixing ratio in the plume of the respective trace gas, 17 is the molar mass of $NH_3$ (in g $mol^{-1}$), and 12 is the molar mass of carbon (in g $mol^{-1}$). $F_c$ is the fraction of carbon in the fuel, which is typically in the 0.45-to-0.55 range

A problem in the calculation of $EF_{NH_3}$ arises from the fact that $NH_3$ is a "sticky" compound. When the aircraft first penetrates a smoke plume, $NH_3$ molecules typically adsorb onto inlet and instrumental surfaces, thereby delaying the signal response of the analyzer. When the airplane exits the plume, the desorbing $NH_3$ molecules cause a signal tailing (Fig.ure S2aa). For calculating $\Delta$, we thus applied the method described in the Supplement of Müller et al. (2016) and calculated cumulative volume mixing ratios including the immediate period (10 s) before the plume was encountered (background) and the period after the plume encounter (seconds to minutes) when the $NH_3$ signal tailed off (Fig.ure S2b). The signal tailing was particularly pronounced during the initial phase of the campaign (before 24 August 2019) when the inlet configuration had not yet been optimized. During the later phase of the campaign, only a few seconds of tailing were observed. $NH_x$ is the sum of $NH_3$ and $NH_4^+$; $EF_{NH_x}$ was calculated as the sum of $EF_{NH_3}$ and $EF_{NH_4^+}$. The modified combustion efficiency (MCE) was calculated as $\Delta CO_2/(\Delta CO_2+\Delta CO)$.
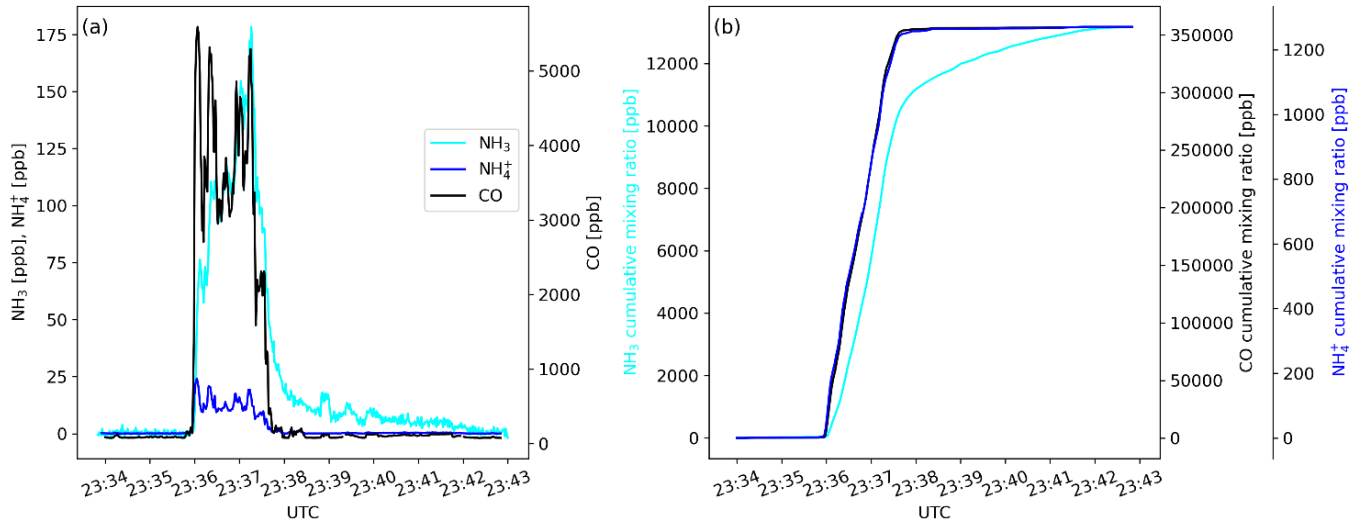
**Figure 2: Time traces of (a) mixing ratios of $NH_3$, $NH_4^+$, and CO and of (b) cumulative mixing ratios of $NH_3$, $NH_4^+$, and CO as measured during a transect of the Williams Flats fire plume on 7 August 2019.**

Data from 180 plume transects were included in our analysis of the wildfire emissions. We only used data from plume transects in which CO mixing ratios exceeded 300 ppb for more than 20 seconds and from plumes in which MCE values were stable (standard deviation of MCE < 0.05). Data from seven plume transects were excluded due to missing $NH_3$, $NH_4^+$ or $CH_4$ data. Our EF analysis was not based on a single plume transect in closest proximity to the wildfire, as we observed in several plumes that $\Delta NH_3/\Delta CO$ increased during a few initial downwind transects (see Fig. S3).
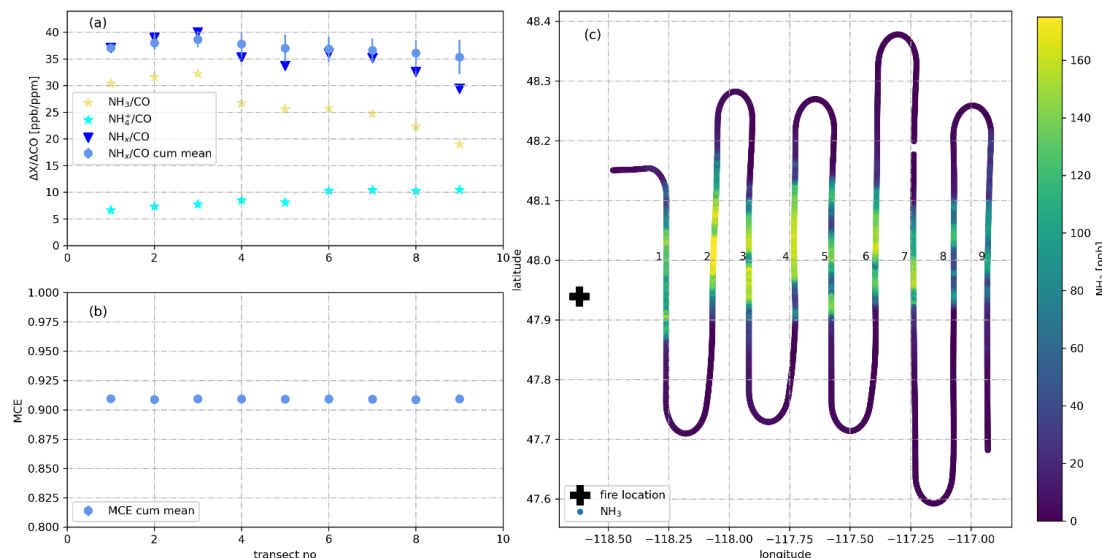
**Figure 3: (a) NH₃/CO, NH₄⁺/CO, NHₓ/CO and cumulative mean NHₓ/CO as measured during nine downwind transects of the plume emitted from the Williams Flats Fire on 7 August 2019. NH₃/CO increases during the first three transects which were thus used for determining $EF_{NH_3}$ and $EF_{NH_x}$. (b) Mean MCE as measured for the same nine downwind transects. MCE remains stable at ~0.91 indicating stable burning conditions. (c) Lat/lon plot showing the location of the fire (black cross) and the flight track color-coded in the NH₃ mixing ratio.**

The reason for this increase (typically <15 %) is unclear. We ~~thus~~ included all plume transects in our analysis, up to where $\Delta NH_3/\Delta CO$ reached its maximum and derived an average $EF_{NH_3}$ and $EF_{NH_x}$ (± standard deviation, SD). All SDs reported herein only reflect the measured variability and do not include measurement uncertainties in the underlying variables (NH₃, NH₄⁺, CO₂, CO, CH₄). Data from 164 plume transects were included in our analysis of the agricultural fire emissions. Data from 12 plume transects were excluded due to missing NH₃ or NH₄⁺ data.

## 3 Results and Discussion

### 3.1 Airborne measurements of NH₃ in smoke plumes

Fig.~~ure 4~~1a shows the mixing ratio of NH₃ ~~(in red)~~ as measured by the PTR-ToF-MS instrument on 7 August 2019 aboard the NASA DC-8. The aircraft flew nine downwind transects at an altitude of 5160 m above sea level (ASL) for sampling the plume emitted from the Williams Flats Fire in Washington State. The NH₃ signal increased with CO ~~(in black)~~ when the plane entered the plume, exhibited a similar time trend as CO within the plume and decreased to background levels outside the plume, although with some tailing (few minutes). NH₃ maxima ranged from 110 to 200 ppb, which were typical maximum NH₃ levels measured in fire plumes throughout the 2019 FIREX-AQ field campaign. Also shown in Fig.~~ure 4~~1a is the time trace of NH₄⁺

(in dark yellow) as measured by the AMS instrument, with maximum mixing ratios ranging from 42 to 65 ppb. The observation of significant amounts of $NH_4^+$ indicates that $NH_4^+$ was primary emitted (as for example observed by Lewis et al., 2009) and/or gaseous $NH_3$ had been partly converted to particulate $NH_4^+$ by the time of sampling ($\geq$2 h after emission). A rapid conversion can be caused by the fast reaction of $NH_3$ with primary emitted acids such as hydrochloric acid (HCl), nitric acid ($HNO_3$) and organic acids, or occur more slowly downwind via the reaction of $NH_3$ with secondary formed acids. As stated in section 2.2, the $NH_4^+$ measurement suffered from a minor ($\leq$ 20%) positive interference from reduced organic nitrogen compounds.

Fig. ~~ure~~ 4~~1~~b shows the mixing ratios of $NH_3$, $NH_4^+$ and CO as observed when the NASA DC-8 crossed a plume emitted from a small cornfield fire in the Mississippi River Valley on 26 August 2019 at an altitude of 325 m ASL. All data are shown at the frequency they were recorded (5 Hz), which resulted in an increased noise for $NH_3$. The tailing was however reduced to a few seconds with the improved PTR-ToF-MS inlet. We show the 5-Hz data for demonstrating that we succeeded in measuring such small fire plumes from a jet aircraft. For further analysis, we used the 1 second integrated data. Notably, the AMS instrument detected significant amounts of $NH_4^+$ in this very fresh plume, indicating that either direct emission from the fire or a rapid conversion of $NH_3$ to $NH_4^+$ had occurred. The latter could be caused by the fast reaction of $NH_3$ with HCl, which is emitted in significant amounts from agricultural fires (Liu et al., 2017). Another plausible explanation is the resuspension of recently applied ammonium nitrate fertilizer.
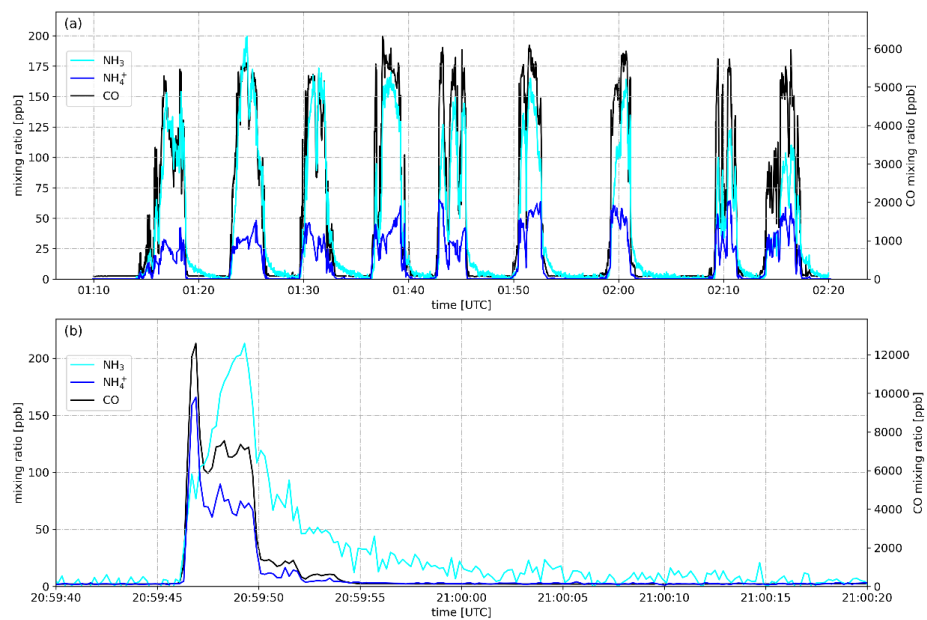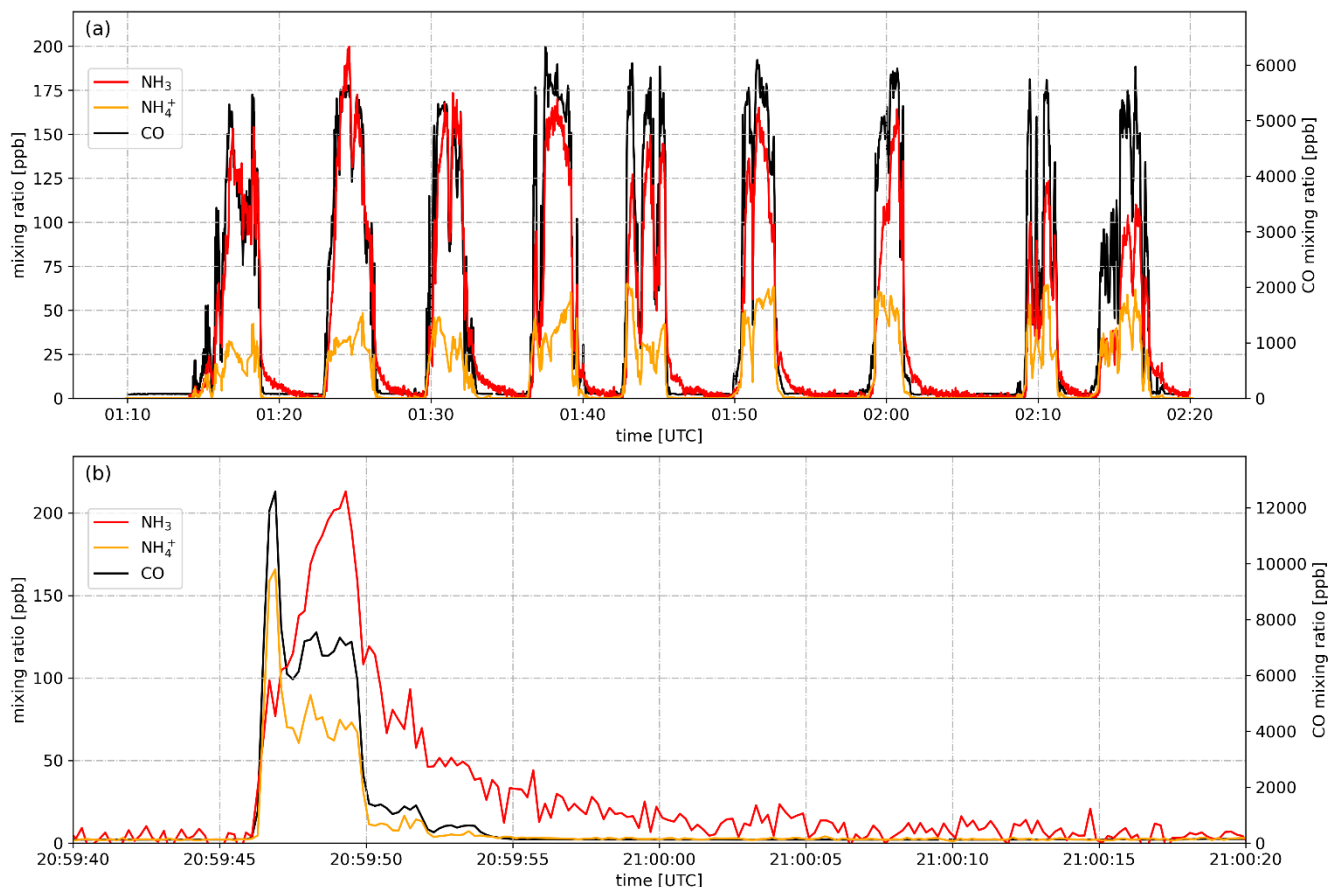
**Figure 14: Mixing ratios of NH₃, NH₄⁺, and CO as measured when the NASA DC-8 transected (a) the plume emitted from the Williams Flats Fire on 7 August, 2019 in downwind direction and (b) the plume emitted from a small corn field fire in the Mississippi River Valley on 26 August, 2019.**

Due to the fact that $NH_4^+$ was already present in very fresh smoke (due to direct emission or rapid conversion), we will herein also report $EF_{NH_x}$, as suggested in previous work by Hegg et al. (1990). In Figure 52a, we plot $EF_{NH_x}$ against $EF_{NH_3}$ for the six Western US wildfires investigated during the 2019 FIREX-AQ field campaign. The two EFs are highly correlated ($R^2$ = 0.96), with the slope of the linear regression curve being close to unity (1.07 ± 0.05). This regression analysis suggests that $NH_4^+$ added ~0.5 g kg$^{-1}$ (offset of the regression line: 0.47 ± 0.11) to $EF_{NH_x}$ throughout the campaign. The offset may be interpreted as the typical direct $NH_4^+$ emission factor (or fast conversion of $NH_3$).

In the case of the agricultural burns, the NASA DC-8 sampled the plumes in very close proximity to the fires. $EF_{NH_x}$ and $EF_{NH_3}$ had again a regression slope of ~1. The offset was mainly caused by elevated $NH_4^+$ emissions and low $NH_3$ emissions from some of the cornfield fires (Fig. 52b).
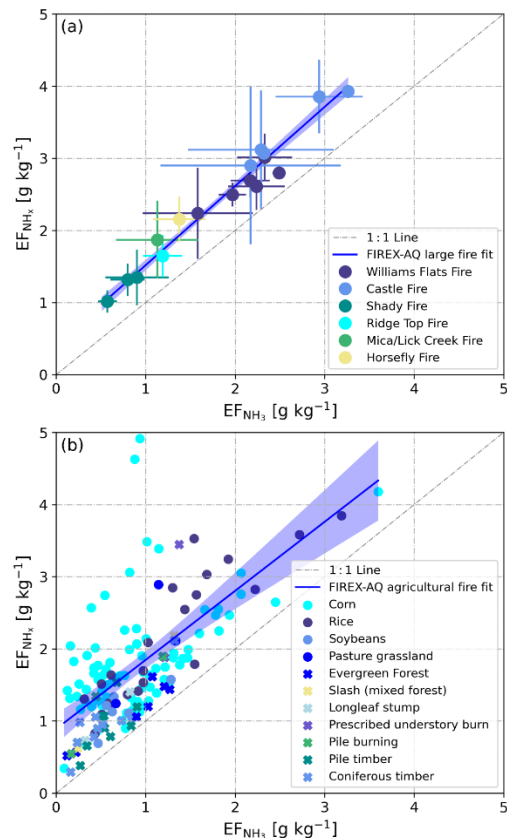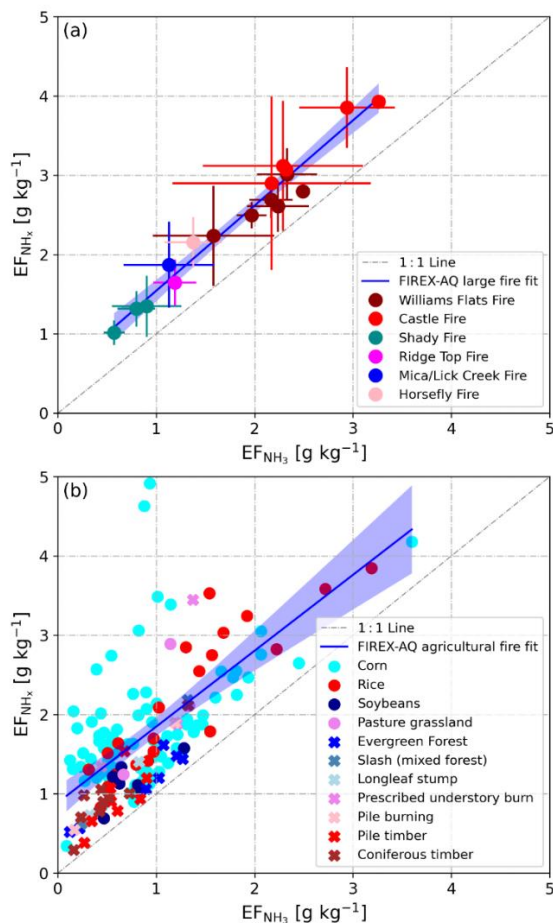
**Figure 2̶5̲:** $EF_{NH_x}$ *vs.* $EF_{NH_3}$ **as derived from** *in situ* **measurements in the plumes of (a) six wildfires and (b) 66 small agricultural fires. In the upper figure, SD bars represent the observed natural variability (measurement uncertainties in NH₃ and NH_x not included). In the lower figure, circles represent field-dominated fuels and crosses represent timber-dominated fuels (see section 3.3). The blue lines represent linear regression curves of the average values for wildfires (a) and of all agricultural data in (b). Shaded areas are 95% confidence bands.**

~~(circles: field-dominated fuels, crosses: timber-dominated fuels; see section 3.3 for details)~~

### 3.2 NH₃ and NH_x emissions from wildfires in the Western US

*In situ* measurements of NH₃ and NH₄⁺ were made in smoke plumes emitted from six wildfires in the Western US. Tab.̶l̶e̶ 1 provides a detailed overview of $EF_{NH_3}$ and $EF_{NH_x}$ derived from these measurements. Plumes from the Shady, Williams Flats and Castle Fires were sampled multiple times and we list the data from each of the sampling patterns as well as the average

value. $EF_{NH_3}$ and $EF_{NH_x}$ were lowest for the Shady Fire. The low emissions may be caused by the difference in fuels, which in the case of the Shady Fire was modified or managed xeric understory (see Tab. S1).

**Table 1:** $EF_{NH_3}$ and $EF_{NH_x}$ derived from *in situ* measurements in the plumes of 6 wildfires in the Western US.

| Name | State | Date (dy.mo.yr) | $EF_{NH_3}$ (g kg⁻¹) mean | SD | $EF_{NH_x}$ (g kg⁻¹) mean | SD | MCE mean | SD |
|---|---|---|---|---|---|---|---|---|
| Shady 1st pattern | ID | 25.07.2019 | 0.57 | 0.11 | 1.02 | 0.15 | 0.906 | 0.003 |
| Shady 2nd pattern | ID | 25.07.2019 | 0.80 | 0.19 | 1.32 | 0.23 | 0.892 | 0.007 |
| Shady 3rd pattern | ID | 25.07.2019 | 0.90 | 0.35 | 1.35 | 0.39 | 0.887 | 0.029 |
| **Shady mean** | | | **0.76** | **0.22** | **1.23** | **0.26** | **0.895** | **0.013** |
| Williams Flats 1st pattern | WA | 03.08.2019 | 1.58 | 0.62 | 2.24 | 0.63 | 0.908 | 0.003 |
| Williams Flats 2nd pattern | WA | 03.08.2019 | 2.24 | 0.32 | 2.61 | 0.33 | 0.907 | 0.005 |
| Williams Flats | WA | 06.08.2019 | 2.33 | 0.31 | 3.01 | 0.33 | 0.894 | 0.004 |
| Williams Flats 1st pattern | WA | 07.08.2019 | 2.49 | 0.07 | 2.80 | 0.09 | 0.905 | 0.004 |
| Williams Flats 2nd pattern | WA | 07.08.2019 | 1.97 | 0.15 | 2.50 | 0.16 | 0.909 | 0.001 |
| Williams Flats 3rd pattern | WA | 07.08.2019 | 2.17 | -- | 2.69 | -- | 0.901 | 0.001 |
| **Williams Flat mean** | | | **2.13** | **0.28** | **2.64** | **0.29** | **0.904** | **0.003** |
| Castle 1st pattern | AZ | 12.08.2019 | 2.29 | 0.81 | 3.12 | 0.82 | 0.884 | 0.003 |
| Castle 2nd pattern | AZ | 12.08.2019 | 2.94 | 0.49 | 3.85 | 0.51 | 0.890 | 0.002 |
| Castle longitudinal transect | AZ | 12.08.2019 | 2.32 | -- | 3.07 | -- | 0.864 | -- |
| Castle 1st pattern | AZ | 13.08.2019 | 2.17 | 1.01 | 2.90 | 1.09 | 0.895 | 0.007 |
| Castle 2nd pattern | AZ | 13.08.2019 | 3.26 | -- | 3.93 | -- | 0.892 | -- |
| **Castle mean** | | | **2.60** | **0.77** | **3.37** | **0.81** | **0.885** | **0.004** |
| Ridge Top | MT | 02.08.2019 | 1.19 | 0.22 | 1.65 | 0.29 | 0.940 | 0.011 |
| Mica/Lick Creek | ID | 02.08.2019 | 1.13 | 0.46 | 1.87 | 0.54 | 0.913 | 0.021 |
| Horsefly | MT | 06.08.2019 | 1.38 | 0.29 | 2.15 | 0.32 | 0.859 | 0.010 |

Average $EF_{NH_3}$ and $EF_{NH_x}$ values for the six wildfires in the Western US were $1.86 \pm 0.75$ g kg⁻¹ and $2.47 \pm 0.80$ g kg⁻¹, respectively. We compare our results to those obtained in two recent studies. Lindaas et al. (2021) investigated $NH_3$ emissions from wildfires in the Western US during the 2018 WE-CAN campaign. We calculated an average $EF_{NH_3}$ of $1.48 \pm 0.91$ g kg⁻¹ for the WE-CAN data. This is slightly lower than the average $EF_{NH_3}$ reported herein, but within the combined uncertainties of the two methods: ±12% for the quantum-cascade tunable infrared laser direct absorption spectrometer (QC-TILDAS) used during WE-CAN, and ±15% for the PTR-ToF-MS analyzer used during FIREX-AQ. Selimovic et al. (2018) investigated emissions from fires fueled by a wide range of US vegetation types in the FIREX FireLab 2016 laboratory study. We only used the data for FIREX-AQ relevant fuels (see Tab. S1) and obtained a significantly lower average $EF_{NH_3}$ of $0.67 \pm 0.38$ g

240    kg$^{-1}$ for the FIREX FireLab data. This finding seems to confirm that laboratory fires do not realistically simulate wildfires (*e.g.*, Yokelson et al., 2013, Hodshire et al., 2019) and thereby underestimate real-world emissions of NH$_3$.

In Fig.~~ure~~ 6~~3~~, we plot the measured $EF_{NH_3}$ values (6 wildfires, multiple sampling of 3 fires) as a function of MCE along with trends from the WE-CAN and FIREX FireLab studies. In the case of the FIREX-AQ data (regression line and confidence band in blue), $EF_{NH_3}$ and MCE correlated poorly, with Pearson's coefficient of determination ($R^2$) being only 0.04. As opposed to

245    the WE-CAN study (regression line and confidence band in black) and the FIREX FireLab experiments (regression line and confidence band in ~~dark yellow~~green), we did not find a clear inversion correlation between MCE and NH$_3$ emissions.
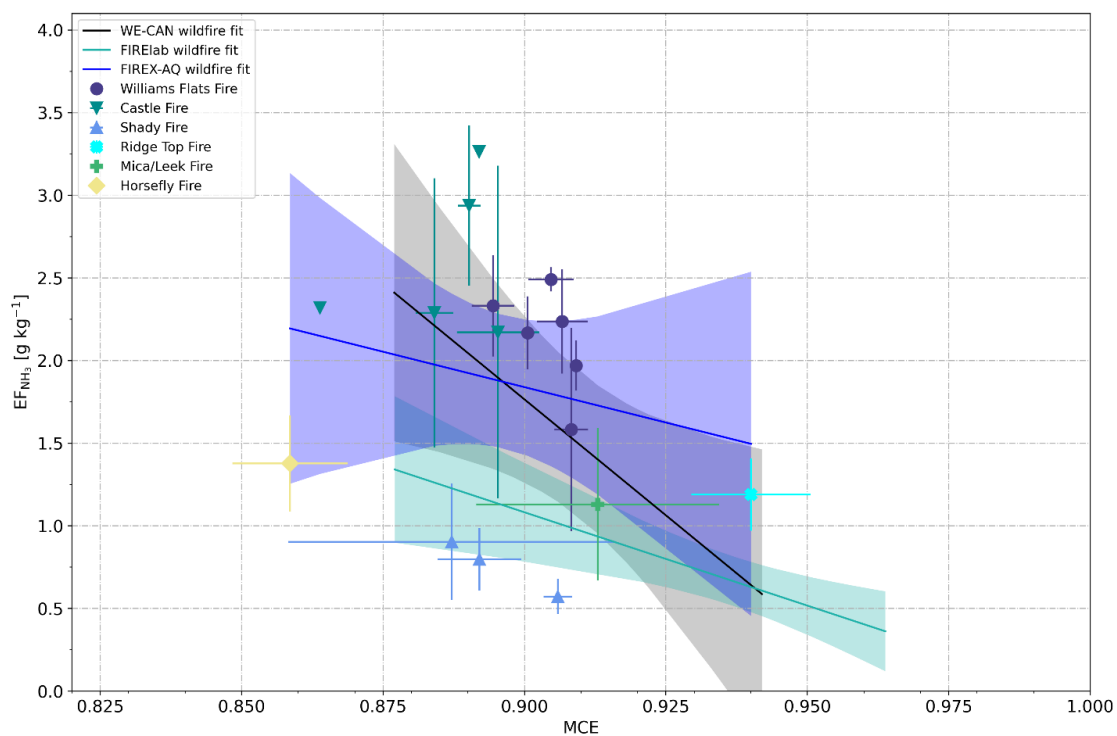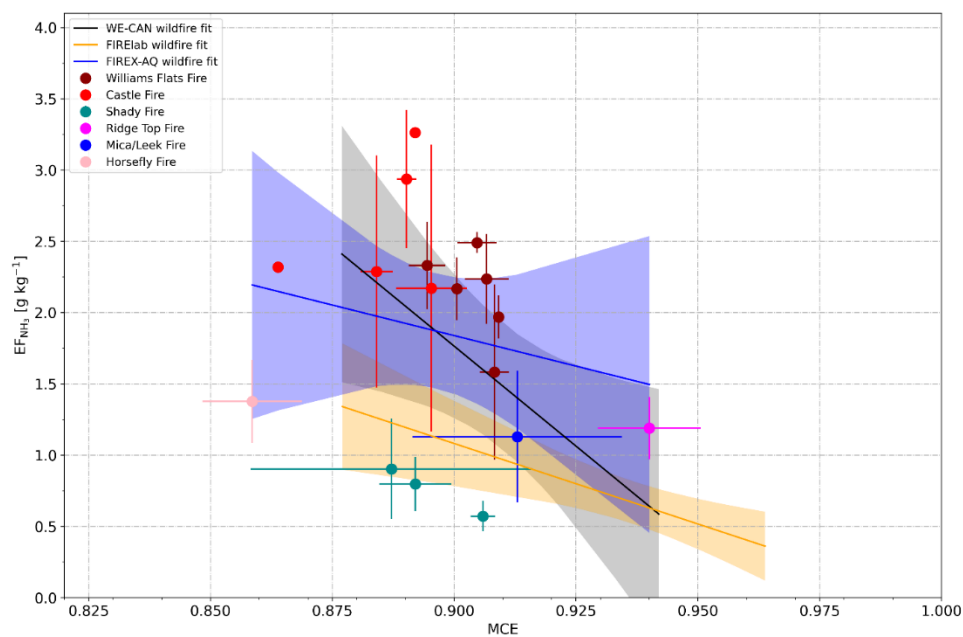
**Figure 63: Scatter plot of $EF_{NH_3}$ (as measured for six Western US wildfires during FIREX-AQ and obtained from two literature sources) *vs.* MCE.**

### 3.3 NH₃ and NHₓ emissions from agricultural fires in the Southeastern US

*In situ* measurements of NH₃ and NH₄⁺ were made in smoke plumes emitted from 66 small agricultural fires in the Southeastern US. $EF_{NH_3}$ values varied widely, covering a range from 0.09 to 3.60 g kg$^{-1}$. The following average values and standard deviations were derived: $EF_{NH_3} = 0.89 \pm 0.58$ g kg$^{-1}$, $EF_{NH_x} = 1.74 \pm 0.92$ g kg$^{-1}$, MCE = 0.92 ± 0.04.

We grouped the agricultural fuels into field-dominated and timber-dominated fuels. The field-dominated fuels include corn, rice, soybeans, and grassland pasture. The timber-dominated fuels include evergreen forest, coniferous timber, prescribed understory fire, pile burning, slash burning, pile timber slash mixture burns, and pile burning of longleaf pine tree stumps. Table 2 lists $EF_{NH_3}$, $EF_{NH_x}$ and MCE for the two main categories and 11 subcategories.

**Table 2: $EF_{NH_3}$, $EF_{NH_x}$ and MCE as measured during FIREX-AQ for small agricultural fires in the Southeastern US burning on different types of fuel.**

| Fuel type | 66 | $EF_{NH_3}$ (g kg$^{-1}$) | | $EF_{NH_x}$ (g kg$^{-1}$) | | MCE | |
|---|---|---|---|---|---|---|---|
| | | mean | SD | mean | SD | mean | SD |
| Corn | 33 | 0.90 | 0.58 | 1.85 | 0.78 | 0.937 | 0.023 |
| Rice | 11 | 1.21 | 0.74 | 2.13 | 0.93 | 0.897 | 0.057 |
| Soybean | 4 | 0.75 | 0.27 | 1.16 | 0.27 | 0.925 | 0.024 |
| Grassland Pasture | 2 | 1.05 | 0.34 | 2.08 | 0.82 | 0.824 | 0.109 |
| **Field-dominated average** | **50** | **0.95** | **0.60** | **1.92** | **0.92** | **0.926** | **0.042** |
| Evergreen Forest | 1 | 0.83 | 0.47 | 1.13 | 0.44 | 0.914 | 0.027 |
| Pile burning (mixed) | 4 | 0.51 | 0.47 | 1.12 | 0.62 | 0.920 | 0.042 |
| Slash burn (mixed forest) | 2 | 0.78 | 0.76 | 1.40 | 1.10 | 0.918 | 0.063 |
| Prescribed understory burn | 1 | 1.39 | 0.19 | 2.67 | 1.11 | 0.864 | 0.022 |
| Pile timber slash | 5 | 0.58 | 0.21 | 0.95 | 0.33 | 0.858 | 0.060 |
| Pile longleaf pine tree stump | 1 | 0.57 | 0.35 | 1.07 | 0.48 | 0.877 | 0.004 |
| Timber slash coniferous | 2 | 0.51 | 0.35 | 0.98 | 0.49 | 0.912 | 0.019 |
| **Timber-dominated average** | **16** | **0.67** | **0.42** | **1.19** | **0.68** | **0.896** | **0.045** |

The data listed in Tab.~~le~~ 2 indicate that field-dominated fuels emit more $NH_3$ and $NH_x$ than timber-dominated fuels. Agricultural areas are usually nitrogen-fertilized, which may cause increased $NH_3$ emissions. $EF_{NH_x}$ is roughly a factor of two higher than $EF_{NH_3}$, which indicates higher primary $NH_4^+$ emissions and/or a very rapid $NH_3$ to $NH_4^+$ conversion in these fresh plumes.

Fig.~~ure~~ 7_4 shows $EF_{NH_3}$ as a function of MCE for different fuels (as measured in individual fires), the averages derived for field-dominated fuels and timber-dominated fuels and the results from four previous studies (McMeeking et al., 2009; Stockwell et al., 2015; Müller et al., 2016; Selimovic et al., 2018). Also in this case, $EF_{NH_3}$ and MCE correlated poorly with $R^2$ being 0.05. The literature values match the low $NH_3$ emissions ($< 1$ g kg$^{-1}$) we observed for most agricultural fires, but the high $NH_3$ emissions from burning rice and corn residues have not been reported before.
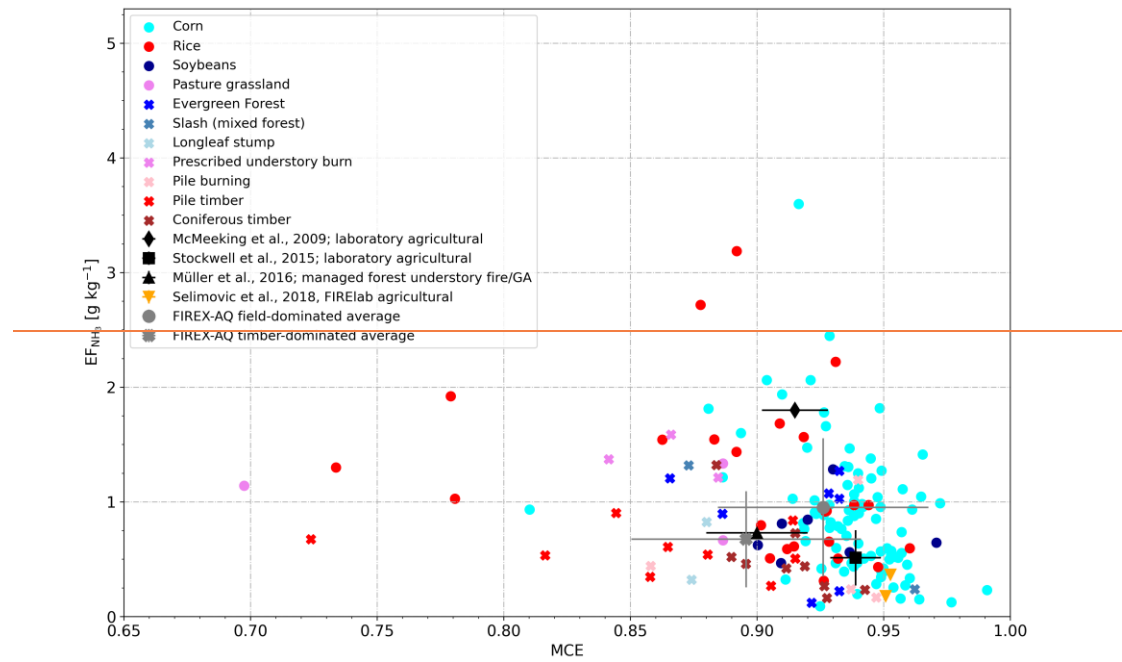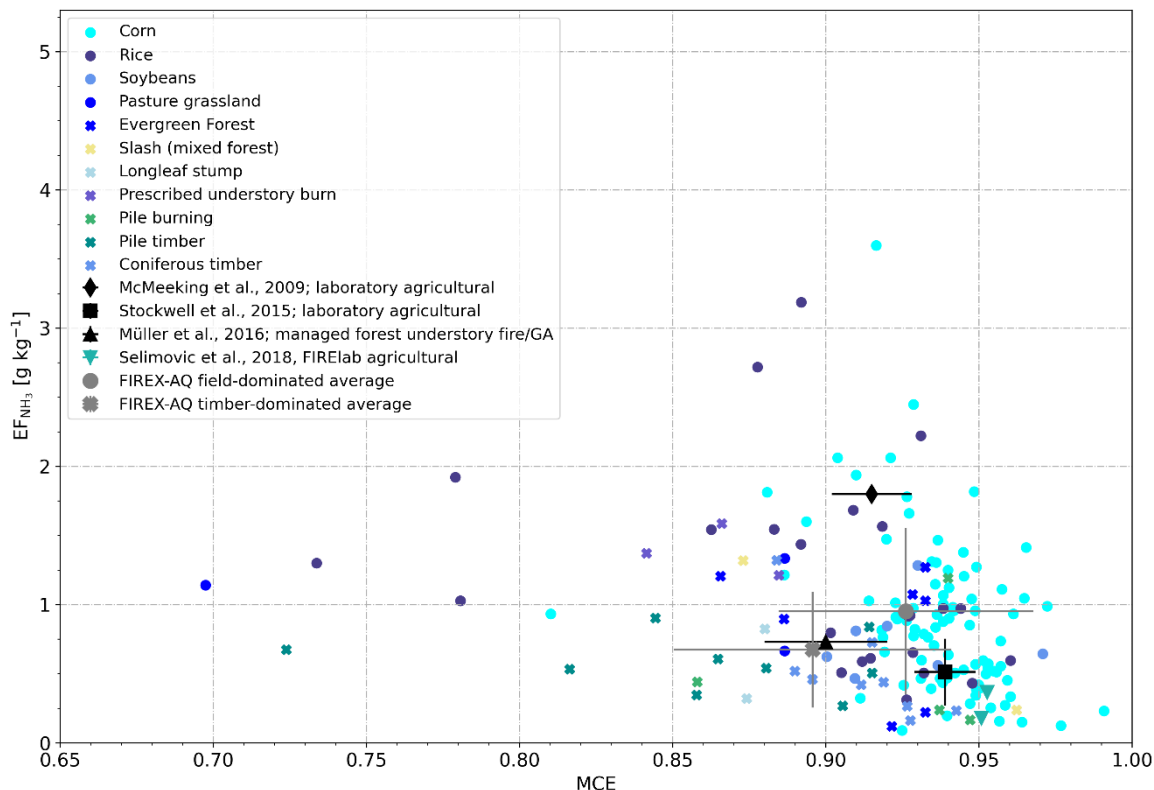
**Figure 74: Scatter plot of $EF_{NH_3}$ vs. MCE as measured for 66 agricultural fires (circles: field-dominated fuels, crosses:**
**timber-dominated fuels) and obtained from four literature sources.**

### 3.4 NH₃ and NHₓ emissions from other fires

We also measured NH₃ and NH₄⁺ in smoke plumes emanating from two prescribed grassland fires in the Central US and one prescribed forest fire in the Southern US. These fires do not fall within the two main categories discussed in the previous two sections and are thus separately presented here. Tab. 3 lists the fire details, $EF_{NH_3}$, $EF_{NH_x}$ and MCE for these three fires.

**Table 3: $EF_{NH_3}$, $EF_{NH_x}$ and MCE as measured during FIREX-AQ for two prescribed grassland fires in the Central US and one prescribed forest fire in the Southern US.**

| Fire details | $EF_{NH_3}$ (g kg⁻¹) | | $EF_{NH_x}$ (g kg⁻¹) | | MCE | |
|---|---|---|---|---|---|---|
| | mean | SD | mean | SD | mean | SD |
| Hickory Ridge State Wildlife Management Area prescribed, 29.08.2019, NE grass during the green growing season (not dry) | 0.33 | 0.12 | 1.19 | 0.93 | 0.907 | 0.002 |
| Tallgrass Prairie National Preserve prescribed, 29.08.2019, KS prairie tallgrass during the green growing season (not dry) | 0.92 | 0.20 | 1.73 | 0.49 | 0.894 | 0.014 |
| Black Water River State Forest prescribed, 30.08.2019, FL oak, mature longleaf pine, mesic and xeric shrub, grass, litter, understory | 0.30 | 0.16 | 0.61 | 0.20 | 0.942 | 0.006 |

## 4 Conclusions

During the 2019 FIREX-AQ field campaign, we measured $NH_3$ and $NH_4^+$ aboard the NASA DC-8 in wildfire and agricultural fire plumes. We found that $NH_4^+$ was either directly emitted from the fire (consistent with past laboratory experiments) and/or $NH_3$ had already partially partitioned to particulate $NH_4^+$ at the time of sampling. We thus also evaluated emissions of $NH_x$ and produced a comprehensive set of $EF_{NH_3}$ and $EF_{NH_x}$ for wildfires in the Western US and agricultural fires in the Southeastern US. Our data show no clear inverse correlation between MCE and $EF_{NH_3}$. $EF_{NH_3}$ values measured in plumes of large wildfires were similar to those observed during the 2018 WE-CAN field campaignmeasurements of past field studies, but significantly higher than observed in the FIREX FireLab 2016 laboratory study. in prior work on laboratory simulated fires, which typically burn on a single fuel. We also report the first extensive set of field measurement derived $EF_{NH_3}$ and $EF_{NH_x}$ values for different types of agricultural fires in the Southeastern US. $NH_3$ emissions were highest from fires of corn and rice residues, which may be caused by fertilization of these fields. Substantial amounts of $NH_4^+$ were detected in freshly emitted smoke from some of the corn and rice field fires, which warrants further investigation.

## Data availability

All the FIREX-AQ data are available at NASA's Atmospheric Science Data Center (DOI: 10.5067/SUBORBITAL/FIREXAQ2019/DATA001) (NASA, 2019).

## Author contribution

LT supported the PTR-ToF-MS instrument development, performed the field measurements, performed the data analysis and interpretation, and wrote the manuscript draft. TM built and characterized the modified PTR-ToF-MS instrument and performed field measurements. FP performed field and laboratory measurements and supported the data analysis as well as the PTR-ToF-MS instrument development. CJN supported the post-mission calibration experiments. PCJ, HG, BAN, MSK and JLJ provided the $NH_4^+$ data. HH, GD, JPD, JBN provided the $CO_2$, CO and $CH_4$ data. EBW, EG and AJS provided the fuel characterization information. AW conceived the modified PTR-ToF-MS instrument, supervised the measurements and data analysis, performed field measurements and finalized the manuscript. All authors commented and accepted the final version of the manuscript.

## Conflicts of interest

The authors declare no conflict of interest.

## Acknowledgements

Laura Tomsche's research was supported by an appointment to the NASA Postdoctoral Program at the NASA Langley Research Center, administered by Universities Space Research Association under contract with NASA. The FIREX AQ project was funded by the NASA Tropospheric Composition Program (TCP). The University of Innsbruck PTR-ToF-MS instrument was partially funded by the Austrian Federal Ministry for Transport, Innovation and Technology (bmvit, FFG, ASAP). FP received funding from the European Union's Horizon 2020 research and innovation program under grant agreement no. 674911 (IMPACT). PCJ, HG, BAN, MKS, and JLJ were supported by NASA Grants 80NSSC18K0630 and 80NSSC21K1451.

## References

Akagi, S. K., Yokelson, R. J., Wiedinmyer, C., Alvarado, M. J., Reid, J. S., Karl, T., Crounse, J. D., Wennberg, P. O.: Emission factors for open and domestic biomass burning for use in atmospheric models, Atmos. Chem. Phys., 11, 4039-4072, 10.5194/acp-11-4039-2011, 2011.

Andreae, M. O.: Emission of trace gases and aerosols from biomass burning – an updated assessment, Atmos. Chem. Phys., 19, 8523-8546, 10.5194/acp-19-8523-2019, 2019.

Andreae, M. O. and Merlet, P.: Emission of trace gases and aerosols from biomass burning, Global biogeochemical cycles, 15, 955-966, https://doi.org/10.1029/2000GB001382, 2001.

Bahreini, R., Ervens, B., Middlebrook, A. M., Warneke, C., de Gouw, J. A., DeCarlo, P. F., Jimenez, J. L., Brock, C. A., Neuman, J. A., Ryerson, T. B., Stark, H., Atlas, E., Brioude, J., Fried, A., Holloway, J. S., Peischl, J., Richter, D., Walega, J., Weibring, P., Wollny, A. G., Fehsenfeld, F. C.: Organic aerosol formation in urban and industrial plumes near Houston and Dallas, Texas, Journal of Geophysical Research: Atmospheres, 114, https://doi.org/10.1029/2008JD011493, 2009.

Bobbink, R. and Hicks, W. K.: Factors Affecting Nitrogen Deposition Impacts on Biodiversity: An Overview, in: Nitrogen Deposition, Critical Loads and Biodiversity, edited by: Sutton, M. A., Mason, K. E., Sheppard, L. J., Sverdrup, H., Haeuber, R., and Hicks, W. K., Springer Netherlands, Dordrecht, 127-138, 10.1007/978-94-007-7939-6_14, 2014.

Burling, I. R., Yokelson, R. J., Griffith, D. W. T., Johnson, T. J., Veres, P., Roberts, J. M., Warneke, C., Urbanski, S. P., Reardon, J., Weise, D. R.: Laboratory measurements of trace gas emissions from biomass burning of fuel types from the southeastern and southwestern United States, Atmos. Chem. Phys., 10, 11115-11130, 10.5194/acp-10-11115-2010, 2010.

Canagaratna, M. R., Jayne, J.T., Jimenez, J.L., Allan, J.D., Alfarra, M.R., Zhang, Q., Onasch, T.B., Drewnick, F., Coe, H., Middlebrook, A., Delia, A., Williams, L.R., Trimborn, A.M., Northway, M.J., DeCarlo, P.F., Kolb, C.E., Davidovits, P., Worsnop, D.R.: Chemical and microphysical characterization of ambient aerosols with the aerodyne aerosol mass spectrometer, Mass Spectrometry Reviews, 26, 185-222, https://doi.org/10.1002/mas.20115, 2007.

DeCarlo, P. F., Kimmel, J. R., Trimborn, A., Northway, M. J., Jayne, J. T., Aiken, A. C., Gonin, M., Fuhrer, K., Horvath, T., Docherty, K. S., Worsnop, D. R., Jimenez, J. L.: Field-Deployable, High-Resolution, Time-of-Flight Aerosol Mass Spectrometer, Analytical Chemistry, 78, 8281-8289, 10.1021/ac061249n, 2006.

Goode, J. G., Yokelson, R. J., Susott, R. A., and Ward, D. E.: Trace gas emissions from laboratory biomass fires measured by open-path Fourier transform infrared spectroscopy: Fires in grass and surface fuels, Journal of Geophysical Research: Atmospheres, 104, 21237-21245, https://doi.org/10.1029/1999JD900360, 1999.

Gordon, I. E., Rothman, L. S., Hill, C., Kochanov, R. V., Tan, Y., Bernath, P. F., Birk, M., Boudon, V., Campargue, A., Chance, K. V., Drouin, B. J., Flaud, J. M., Gamache, R. R., Hodges, J. T., Jacquemart, D., Perevalov, V. I., Perrin, A., Shine, K. P., Smith, M. A. H., Tennyson, J., Toon, G. C., Tran, H., Tyuterev, V. G., Barbe, A., Csaszar, A. G., Devi, V. M., Furtenbacher, T., Harrison, J. J., Hartmann, J. M., Jolly, A., Johnson, T. J., Karman, T., Kleiner, I., Kyuberis, A. A., Loos, J., Lyulin, O. M., Massie, S. T., Mikhailenko, S. N., Moazzen-Ahmadi, N., Muller, H. S. P., Naumenko, O. V., Nikitin, A. V., Polyansky, O. L., Rey, M., Rotger, M., Sharpe, S. W., Sung, K., Starikova, E., Tashkun, S. A., Vander Auwera, J., Wagner, G., Wilzewski, J., Wcislo, P., Yu, S., and Zak, E. J.: The HITRAN2016 molecular spectroscopic database, J. Quant. Spectrosc. Radiat. Transfer, 203, 3-69, 10.1016/j.jqsrt.2017.06.038, 2017.

Griffith, D. W.: Synthetic calibration and quantitative analysis of gas-phase FT-IR spectra, Applied spectroscopy, 50, 59-70, 1996.

Guo, H., Campuzano-Jost, P., Nault, B. A., Day, D. A., Schroder, J. C., Kim, D., Dibb, J. E., Dollner, M., Weinzierl, B., Jimenez, J. L.: The importance of size ranges in aerosol instrument intercomparisons: a case study for the Atmospheric Tomography Mission, Atmos. Meas. Tech., 14, 3631-3655, 10.5194/amt-14-3631-2021, 2021.

Hegg, D. A., Radke, L. F., Hobbs, P. V., Rasmussen, R. A., Riggan, P.: Emissions of some trace gases from biomass fires, Journal of Geophysical Research: Atmospheres, 95, 5669-5675, https://doi.org/10.1029/JD095iD05p05669, 1990.

Hodshire, A. L., Akherati, A., Alvarado, M. J., Brown-Steiner, B., Jathar, S. H., Jimenez, J. L., Kreidenweis, S. M., Lonsdale, C. R., Onasch, T. B., Ortega, A. M., Pierce, J. R.: Aging Effects on Biomass Burning Aerosol Mass and Composition: A Critical Review of Field and Laboratory Studies, Environmental Science & Technology, 53, 10007-10022, 10.1021/acs.est.9b02588, 2019.

Kelly, J. T., Parworth, C. L., Zhang, Q., Miller, D. J., Sun, K., Zondlo, M. A., Baker, K. R., Wisthaler, A., Nowak, J. B., Pusede, S. E., Cohen, R. C., Weinheimer, A. J., Beyersdorf, A. J., Tonnesen, G. S., Bash, J. O., Valin, L. C., Crawford, J.H., Fried, A., Walega, J.G.: Modeling NH4NO3 Over the San Joaquin Valley During the 2013 DISCOVER-AQ Campaign, Journal of Geophysical Research: Atmospheres, 123, 4727-4745, https://doi.org/10.1029/2018JD028290, 2018.

Lindaas, J., Pollack, I. B., Garofalo, L. A., Pothier, M. A., Farmer, D. K., Kreidenweis, S. M., Campos, T. L., Flocke, F., Weinheimer, A. J., Montzka, D. D., Tyndall, G. S., Palm, B. B., Peng, Q., Thornton, J. A., Permar, W., Wielgasz, C., Hu, L., Ottmar, R. D., Restaino, J. C., Hudak, A. T., Ku, I-T., Zhou, Y., Sive, B. C., Sullivan, A., Collett Jr, J. L., Fischer, E. V.: Emissions of Reactive Nitrogen From Western U.S. Wildfires During Summer 2018, Journal of Geophysical Research: Atmospheres, 126, e2020JD032657, https://doi.org/10.1029/2020JD032657, 2021.

Liu, X., Huey, L. G., Yokelson, R. J., Selimovic, V., Simpson, I. J., Müller, M., and Jimenez, J. L., Campuzano-Jost, P., Beyersdorf, A. J., Blake, D. R., Butterfield, Z., Choi, Y., Crounse, J. D., Day, D. A., Diskin, G. S., Dubey, M. K., Fortner, E., Hanisco, T. F., Hu, W., King, L. E., Kleinman, L., Meinardi, S., Mikoviny, T., Onasch, T. B., Palm, B. B., Peischl, J., Pollack, I. B., Ryerson, T. B., Sachse, G. W., Sedlacek, A. J., Shilling, J. E., Springston, S., St. Clair, J. M., Tanner, D. J., Teng, A. P., Wennberg, P. O., Wisthaler, A., Wolfe, G. M.: Airborne measurements of western U.S. wildfire emissions: Comparison with prescribed burning and air quality implications, Journal of Geophysical Research: Atmospheres, 122, 6108-6129, 10.1002/2016jd026315, 2017.

Lobert, J. M., Scharffe, D. H., Hao, W. M., and Crutzen, P. J.: Importance of biomass burning in the atmospheric budgets of nitrogen-containing gases, Nature, 346, 552-554, 10.1038/346552a0, 1990.

Mace, K. A., Artaxo, P., Duce, R. A.: Water-soluble organic nitrogen in Amazon Basin aerosols during the dry (biomass burning) and wet seasons, Journal of Geophysical Research: Atmospheres, 108(D16), 4512, 10.1029/2003JD003557, 2003.

390    McMeeking, G. R., Kreidenweis, S. M., Baker, S., Carrico, C. M., Chow, J. C., Collett, J. L., Hao, W. M., Holden, A. S., Kirchstetter, T. W., Malm, W. C., Moosmüller, H., Sullivan, A. P., Wold, C. E.: Emissions of trace gases and aerosols during the open combustion of biomass in the laboratory, Journal of Geophysical Research, 114, 10.1029/2009jd011836, 2009.

Müller, M., Mikoviny, T., Feil, S., Haidacher, S., Hanel, G., Hartungen, E., Jordan, A., Märk, L., Mutschlechner, P., Schottkowsky, R.: A compact PTR-ToF-MS instrument for airborne measurements of volatile organic compounds at high
395    spatiotemporal resolution, Atmos. Meas. Tech., 7, 3763-3772, 10.5194/amt-7-3763-2014, 2014.

Müller, M., Mikoviny, T., Feil, S., Haidacher, S., Hanel, G., Hartungen, E., Jordan, A., Märk, L., Mutschlechner, P., Schottkowsky, R., Anderson, B. E., Beyersdorf, A. J., Crawford, J. H., Diskin, G. S., Eichler, P., Fried, A., Keutsch, F. N., Mikoviny, T., Thornhill, K. L., Walega, J. G., Weinheimer, A. J., Yang, M., Yokelson, R. J., Wisthaler, A.: In situ measurements and modeling of reactive trace gases in a small biomass burning plume, Atmos. Chem. Phys., 16, 3813-3824,
400    10.5194/acp-16-3813-2016, 2016.

Müller, M., Piel, F., Gutmann, R., Sulzer, P., Hartungen, E., Wisthaler, A.: A novel method for producing NH4+ reagent ions in the hollow cathode glow discharge ion source of PTR-MS instruments, International Journal of Mass Spectrometry, 447, 116254, https://doi.org/10.1016/j.ijms.2019.116254, 2020.

Nault, B. A., Campuzano-Jost, P., Day, D. A., Jo, D. S., Schroder, J. C., Allen, H. M., Bahreini, R., Bian, H., Blake, D. R.,
405    Chin, M., Clegg, S. L., Colarco, P. R., Crounse, J. D., Cubison, M. J., DeCarlo, P. F., Dibb, J. E., Diskin, G. S., Hodzic, A., Hu, W., Katich, J. M., Kim, M. J., Kodros, J. K., Kupc, A., Lopez-Hilfiker, F. D., Marais, E. A., Middlebrook, A. M., Neuman,A. J., Nowak, J. B., Palm, B. B., Paulot, F., Pierce, J. R., Schill, G. P., Scheuer, E., Thornton, J. A., Tsigaridis, K., Wennberg, P. O., Williamson, C. J., Jimenez, Jose L.: Chemical transport models often underestimate inorganic aerosol acidity in remote regions of the atmosphere, Communications Earth & Environment, 2, 93, 10.1038/s43247-021-00164-0, 2021.

410    Ottmar, R. D., Sandberg, D.V., Riccardi, C. L., Prichard, S.J.: An overview of the Fuel Characteristic Classification System — Quantifying, classifying, and creating fuelbeds for resource planning, Canadian Journal of Forest Research, 37, 2383-2393, 10.1139/x07-077, 2007.

Pan, D., Benedict, K. B., Golston, L. M., Wang, R., Collett, J. L., Tao, L., Sun, K., Guo, X., Ham, J., Prenni, A. J., Schichtel, B. A., Mikoviny, T., Müller, M., Wisthaler, A., Zondlo, M. A.: Ammonia Dry Deposition in an Alpine Ecosystem Traced to
415    Agricultural Emission Hotpots, Environmental Science & Technology, 55, 7776-7785, 10.1021/acs.est.0c05749, 2021.

Piel, F., Müller, M., Winkler, K., Skytte af Sätra, J., and Wisthaler, A.: Introducing the extended volatility range proton-transfer-reaction mass spectrometer (EVR PTR-MS), Atmos. Meas. Tech., 14, 1355-1363, 10.5194/amt-14-1355-2021, 2021.

Prichard, S. J., O'Neill, S. M., Eagle, P., Andreu, A. G., Drye, B., Dubowy, J., Urbanski, S., Strand, T. M.: Wildland fire emission factors in North America: synthesis of existing data, measurement needs and management applications, International
420    Journal of Wildland Fire, 29, 132-147, https://doi.org/10.1071/WF19066, 2020.

Pye, H. O. T., Nenes, A., Alexander, B., Ault, A. P., Barth, M. C., Clegg, S. L., Collett Jr, J. L., Fahey, K. M., Hennigan, C. J., Herrmann, H., Kanakidou, M., Kelly, J. T., Ku, I. T., McNeill, V. F., Riemer, N., Schaefer, T., Shi, G., Tilgner, A., Walker, J. T., Wang, T., Weber, R., Xing, J., Zaveri, R. A., Zuend, A.: The acidity of atmospheric particles and clouds, Atmos. Chem. Phys., 20, 4809-4888, 10.5194/acp-20-4809-2020, 2020.

425    Roberts, J. M., Stockwell, C. E., Yokelson, R. J., de Gouw, J., Liu, Y., Selimovic, V., Koss, A. R., Sekimoto, K., Coggon, M. M., Yuan, B., Zarzana, K. J., Brown, S. S., Santin, C., Doerr, S. H., Warneke, C.: The nitrogen budget of laboratory-simulated western US wildfires during the FIREX 2016 Fire Lab study, Atmos. Chem. Phys., 20, 8807-8826, 10.5194/acp-20-8807-2020, 2020.

Sachse, G., Collins, J., Hill, G., Wade, L., Burney, L., Ritter, J.: Airborne tunable diode laser sensor for high-precision
430    concentration and flux measurements of carbon monoxide and methane, in: Measurement of atmospheric gases, Proc. SPIE, Los Angeles, CA, United States, https://doi.org/10.1117/12.46162, 1991.

Seinfeld, J. H., Pandis, S. N.: Atmospheric Chemistry and Physics: From Air Pollution to Climate Change, John Wiley & Sons2016.

Selimovic, V., Yokelson, R. J., Warneke, C., Roberts, J. M., de Gouw, J., Reardon, J., Griffith, D. W. T.: Aerosol optical
435    properties and trace gas emissions by PAX and OP-FTIR for laboratory-simulated western US wildfires during FIREX, Atmos. Chem. Phys., 18, 2929-2948, 10.5194/acp-18-2929-2018, 2018.

Stockwell, C. E., Veres, P. R., Williams, J., and Yokelson, R. J.: Characterization of biomass burning emissions from cooking fires, peat, crop residue, and other fuels with high-resolution proton-transfer-reaction time-of-flight mass spectrometry, Atmos. Chem. Phys., 15, 845-865, 10.5194/acp-15-845-2015, 2015.

440 Sun, K., Cady-Pereira, K., Miller, D. J., Tao, L., Zondlo, M. A., Nowak, J. B., Neuman, J. A., Mikoviny, T., Müller, M., Wisthaler, A., Scarino, A. J., Hostetler, C. A.: Validation of TES ammonia observations at the single pixel scale in the San Joaquin Valley during DISCOVER-AQ, Journal of Geophysical Research: Atmospheres, 120, 5140-5154, https://doi.org/10.1002/2014JD022846, 2015.

Vay, S. A., Tyler, S. C., Choi, Y., Blake, D. R., Blake, N. J., Sachse, G. W., Diskin, G. S., Singh, H. B.: Sources and transport
445 of Delta14C in CO2 within the Mexico City Basin and vicinity, Atmos. Chem. Phys., 9, 4973-4985, 10.5194/acp-9-4973-2009, 2009.

Warneke, C., J.P. Schwarz, J.E. Dibb, O. Kalashnikova, G. Frost, J. Al-Saadi, S.S. Brown, W.A. Brewer, A. Soja, F.C. Seidel, R.A. Washenfelder, E.B. Wiggins, R.H. Moore, B.E. Anderson, C. Jordan, T.I. Yacovitch, S.C. Herndon, S. Liu, T. Kuwayama, D. Jaffe, N. Johnston, V. Selimovic, R. Yokelson, D.M. Giles, B.N. Holben, P. Goloub, I. Popovici, M. Trainer,
450 Ad. Kumar, R.B. Pierce, D. Fahey, J. Roberts, E.M. Gargulinski, D.A. Peterson, X. Ye, L.H. Thapa, P.E. Saide, C.H. Fite, C.D. Holmes, S. Wang, M.M. Coggon, Z.C.J. Decker, C.E. Stockwell, L. Xu, G. Gkatzelis, K. Aikin, B. Lefer, J. Kaspari, D. Griffin, L. Zeng, R. Weber, M. Hastings, J. Chai, G.M. Wolfe, T.F. Hanisco, J. Liao, P. Campuzano-Jost, H. Guo, J.L. Jimenez, J. Crawford: Fire Influence on Regional to Global Environments and Air Quality (FIREX-AQ), Journal of Geophysical Research: Atmospheres, e2022JD037758, https://doi.org/10.1029/2022JD037758, 2022.

455 Yokelson, R. J., Burling, I. R., Gilman, J. B., Warneke, C., Stockwell, C. E., de Gouw, J., Akagi, S. K., Urbanski, S. P., Veres, P., Roberts, J. M., Kuster, W. C., Reardon, J., Griffith, D. W. T., Johnson, T. J., Hosseini, S., Miller, J. W., Cocker Iii, D. R., Jung, H., Weise, D. R.: Coupling field and laboratory measurements to estimate the emission factors of identified and unidentified trace gases for prescribed fires, Atmos. Chem. Phys., 13, 89-116, 10.5194/acp-13-89-2013, 2013.

Yokelson, R. J., Goode, J. G., Ward, D. E., Susott, R. A., Babbitt, R. E., Wade, D. D., Bertschi, I., Griffith, D. W. T., Hao, W.
460 M.: Emissions of formaldehyde, acetic acid, methanol, and other trace gases from biomass fires in North Carolina measured by airborne Fourier transform infrared spectroscopy, Journal of Geophysical Research: Atmospheres, 104, 30109-30125, https://doi.org/10.1029/1999JD900817, 1999.

Yokelson, R. J., Griffith, D. W. T., Ward, D. E: Open-path Fourier transform infrared studies of large-scale laboratory biomass fires, Journal of Geophysical Research: Atmospheres, 101, 21067-21080, https://doi.org/10.1029/96JD01800, 1996.

465 Yokelson, R. J., Susott, R., Ward, D. E., Reardon, J., Griffith, D. W. T.: Emissions from smoldering combustion of biomass measured by open-path Fourier transform infrared spectroscopy, Journal of Geophysical Research: Atmospheres, 102, 18865-18877, https://doi.org/10.1029/97JD00852, 1997.